

Composite Materials in the Zirconia–Tricalcium Phosphate System for Bone Implants

V. V. Smirnov^a, M. A. Goldberg^{a,*}, A. I. Krylov^a, S. V. Smirnov^a, O. S. Antonova^{a,b}, Yu. B. Tyut'kova^a,
A. A. Kononov^a, L. I. Podzorova^a, and Corresponding Member of the RAS S. M. Barinov^a

Received May 29, 2018

Abstract—Based on tricalcium phosphate, new high-strength composite materials were synthesized, in which the strengthening phase was ZrO₂. To reduce the sintering temperature and obtain a fine crystalline structure, a special additive based on sodium silicate was developed, which favored the formation of low-temperature melts. It was studied how the ratio between the initial components and the sintering conditions affect the phase composition, microstructure, and mechanical properties of the obtained composite materials. By improving technology and optimizing composition, strong ZrO₂-rich composites were produced in the tetragonal modification with a low sintering temperature of 1250–1350°C and a flexural strength to 260 MPa. The composites had microstructure with tricalcium phosphate and ZrO₂ crystal sizes to 500 nm and to 5 μm, respectively. Such materials can be used in medicine for manufacturing bone implants capable of withstanding physiological loads.

DOI: 10.1134/S0012500818110046

Partially stabilized zirconia (PSZ) has high mechanical strength, wear and corrosion resistance, and biocompatibility [1]. PSZ materials are used in medicine as dental materials and materials for hip implants and coatings for endoprostheses [2]. One of the ways to improve the biocompatibility of PSZ materials is to introduce calcium phosphates, which are biocompatible and osteoconductive [3]. Owing to its high mechanical properties, PSZ is used to reinforce bone cements based on calcium phosphates with e.g., PSZ nanoparticles and nanotubes, which increases the compressive strength of cements by up to 50% [4]. Sintered composite ceramic materials in the hydroxyapatite–PSZ system are known [5]. Production of such materials is complicated by the low thermal stability of hydroxyapatite, which additionally decreases in the presence of ZrO₂. It was found [6] that, after adding 3% ZrO₂, the thermal decomposition of hydroxyapatite to form tricalcium phosphate (TCP) begins at as low as 1100°C. The interaction between hydroxyapatite and PSZ gives calcium zirconate and calcium oxide, which limits the sintering temperatures of ceramic materials and prevents the production of high-strength dense sintered samples

[6]. Further advances in creating composite materials in the PSZ–calcium phosphates system can be reached by passing to thermally more stable high-temperature phases, such as TCP. TCP matrices are used to replace and repair bone defects [7]. The creation of a composite material in the PSZ–TCP system is promising owing to the preservation of the phase composition of the initial components, the achievement of high strength characteristics, and the improvement of biological properties.

In this context, the purpose of this work was the synthesis and sintering of new composite materials based on PSZ and TCP over a wide concentration range and the investigation of the formation of their phase composition and microstructure.

EXPERIMENTAL

Partially stabilized zirconia powders were produced by precipitation from aqueous solutions of chemically pure salts ZrOCl₂ · 8H₂O and YCl₃ · 6H₂O to which Y₂O₃ was added to a concentration of 3.5 mol %. The precipitant was 9% aqueous ammonia. After the precipitation, the obtained precipitate was filtered off on a Buchner funnel, dried in a laboratory dryer at 100°C, and then calcined in a muffle furnace at 450°C.

A TCP powder was obtained by precipitation from aqueous solutions by the reaction

^aBaikov Institute of Metallurgy and Materials Science, Russian Academy of Sciences, Moscow, 119991 Russia

^bBlagonravov Institute of Machine Science, Russian Academy of Sciences, Moscow, 101990 Russia

*e-mail: naiv.syper@gmail.com

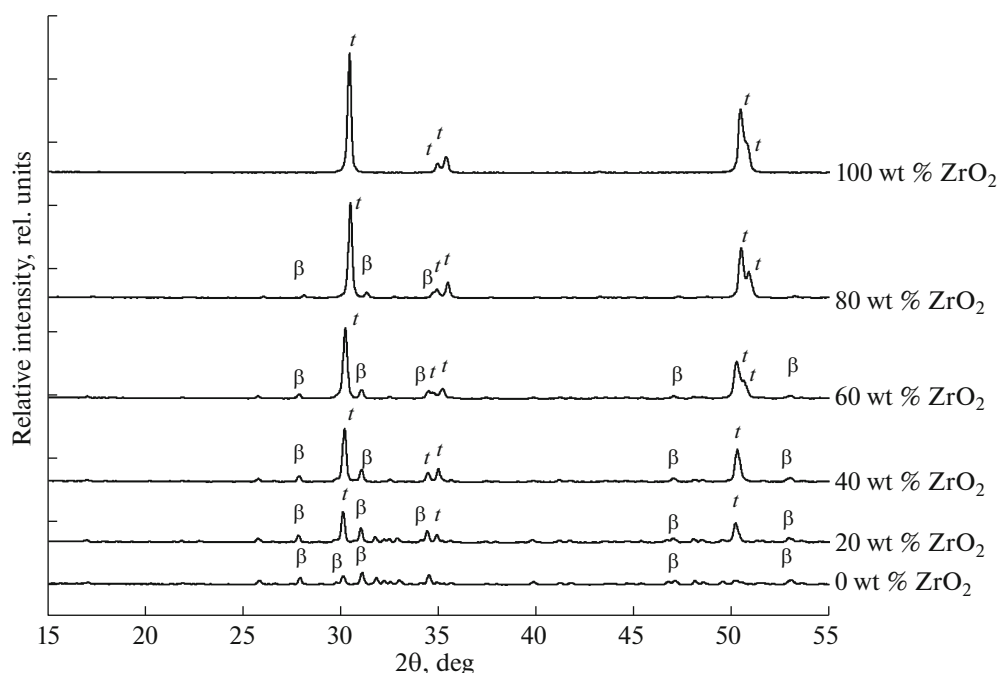
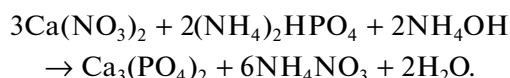


Fig. 1. X-ray powder diffraction patterns of the sintered samples of the ceramics without a Na_2SiO_3 -based additive; *t* indicates the tetragonal modification of ZrO_2 and β , β -tricalcium phosphate.



The pH of the synthesis (6.8–7.4) was maintained by adding aqueous ammonia and acetic acid. The produced precipitate was filtered off on a Buchner funnel and dried at 220°C.

The synthesized TCP and ZrO_2 powders were mixed at ZrO_2 contents from 0 to 100 wt % at an interval of 20 wt % in a planetary mill with Teflon jars and zirconia balls in a dimethyl ketone medium, after which the mixture was filtered off and redried at 200°C. The produced composites were compacted by uniaxial pressing into rectangular samples $30 \times 3 \times 3$ mm in size in steel dies at a specific pressure of 100 MPa. Annealing was carried out in furnaces with silicon carbide heaters at temperatures from 1250 to 1350°C.

To reduce the sintering temperature and obtain a fine crystalline structure, a sintering additive based on sodium silicate was introduced to the powders to a concentration of 5 wt %.

The materials were studied by X-ray powder diffraction analysis with a Shimadzu XRD-6000 diffractometer (Shimadzu, Japan) in CuK_α radiation. The phase composition was identified according to the JCPDS database using an automated system for recording and processing experimental data. The specific surface areas of the obtained ZrO_2 and TCP powders were determined by the BET method with a Micromeritics TriStar 3020 analyzer. The microstruc-

ture of the ceramic materials was studied on a Tescan Vega II scanning electron microscope in secondary electrons at a voltage of 15 kV. The three-point-bending strength was measured on an Instron 5581 universal testing machine using no less than five samples per measurement.

According to the X-ray powder diffraction data, the phase composition of the ZrO_2 powders after heat treatment at 450°C corresponded to a zirconia-based solid solution with a pseudocubic structure. The TCP powder after the synthesis and heat treatment at 220°C consisted of amorphous calcium phosphate with a low degree of crystallinity. The specific surface areas of the ZrO_2 and TCP powders were 85 ± 3 and 80 ± 3 m^2/g , respectively.

The sintering within the temperature range from 1250 to 1350°C showed an increase in the linear shrinkage with increasing sintering temperature for all the compositions. After the sintering, the composite ceramic materials containing no Na_2SiO_3 -based sintering additive consisted of ZrO_2 in the tetragonal modification and TCP with the whitlockite (β -tricalcium phosphate) structure. Figure 1 presents the X-ray powder diffraction patterns of the materials after sintering at 1250°C. It is seen from Fig. 1 that the ratio between the intensities of the main peaks of phases changed in accordance with the change in their calculated concentrations in the composite.

The materials containing the sintering additive were characterized by the formation of the monoclinic phase, the content of which increased with increasing

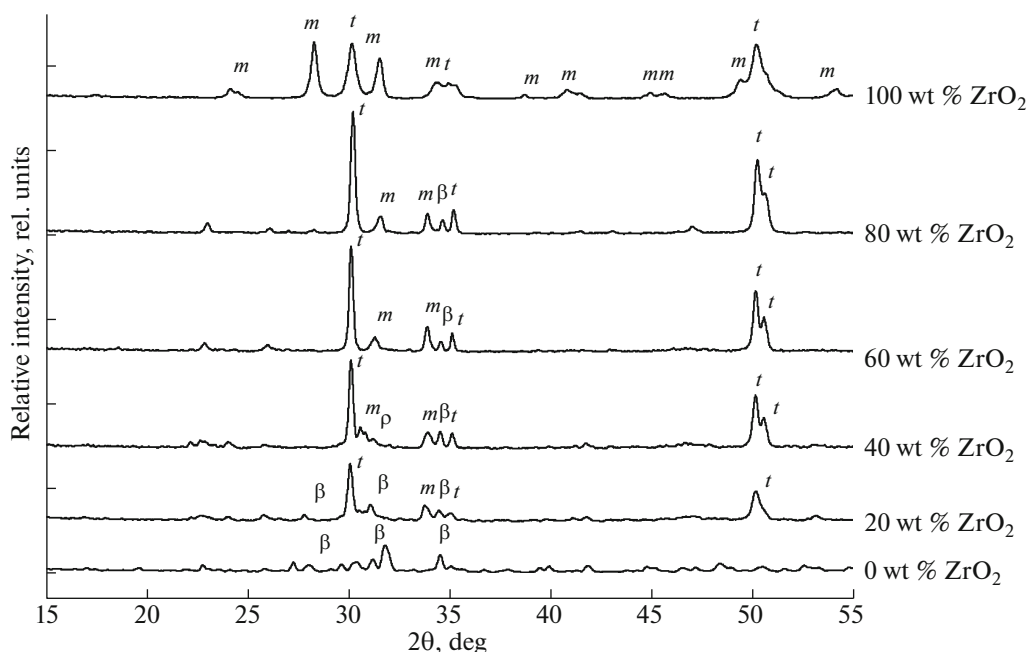


Fig. 2. X-ray powder diffraction patterns of the sintered samples of the ceramics with a Na_2SiO_3 -based additive; *t* indicates the tetragonal modification of ZrO_2 , *m*, the monoclinic modification of ZrO_2 , and β , β -tricalcium phosphate.

ZrO_2 content (Fig. 2). The monoclinic modification forms because Y_2O_3 interacts with Na_2SiO_3 and is released from the ZrO_2 lattice, reducing the degree of stabilization of PSZ. Note that, in the composite containing 80 wt % ZrO_2 , the content of the monoclinic phase did not exceed 15 wt %, whereas in pure ZrO_2 , its content was about 50 wt %. The presence of TCP is likely to favor the preservation of the tetragonal modification of ZrO_2 , which may be due to the partial dissolution of TCP with the incorporation of CaO into the ZrO_2 lattice [8]. A further increase in the sintering temperature to 1350°C promoted an increase in the degree of crystallinity of the main phases, and the content of the monoclinic modification of ZrO_2 increased insignificantly: within 3 wt %.

Further, we studied the microstructure of the composite materials sintered at 1350°C and detected that it changed significantly as ZrO_2 and the sintering additive were added. The materials containing no ZrO_2 had a dense sintered structure with a TCP grain size of about $10\ \mu\text{m}$. The introduction of the sintering additive had no material influence on the microstructure of the ceramics. The addition of ZrO_2 to a concentration of 20 wt % to the materials that contained no sintering additive but contained Na_2SiO_3 gave rise to a microstructure with a porosity of 30%. ZrO_2 grains less than $0.2\ \mu\text{m}$ in size were uniformly distributed over the TCP matrix. The addition of the sintering additive led to an increase in the TCP grain size (Figs. 3a, 3b). With increasing ZrO_2 content to 80 wt %, the structure of the materials without the sintering

additive remained loose and nonuniform, consisting of ZrO_2 grains less than $0.5\ \mu\text{m}$ in size and $5\text{-}\mu\text{m}$ TCP grains. The porosity remained about 15–20% for all the compositions (Fig. 3c). For the materials with the sintering additive, the porosity decreased with a further increase in the ZrO_2 content: it was 5–10% at a ZrO_2 content of 40 wt % and virtually vanished (less than 2%) at ZrO_2 contents of 60 and 80 wt % (Fig. 3d). Such ceramic materials consisted of $0.5\text{-}\mu\text{m}$ ZrO_2 particles and $5\text{--}10\text{-}\mu\text{m}$ TCP particles. The particle size was independent of the concentrations of components. The materials containing 100% ZrO_2 had an inhomogeneous microstructure formed by sintered agglomerates with a porosity to 10% and a ZrO_2 grain size of $0.5\ \mu\text{m}$, regardless of the presence of the sintering additive.

The mechanical testing of the ceramic materials was carried out on samples sintered at 1350°C with a porosity less than 5%. According to the mechanical testing data, the materials containing no ZrO_2 (pure TCP) had a flexural strength of $55 \pm 5\ \text{MPa}$ in the absence of the sintering additive and $63 \pm 5\ \text{MPa}$ in the presence of the sintering additive based on Na_2SiO_3 ; i.e., the strength was virtually independent of the introduction of the additive. The strongest samples were the composite ceramic materials obtained using the sintering additive with a dense uniform structure; namely, the materials containing 60 and 80 wt % ZrO_2 had strengths of 150 ± 5 and $260 \pm 10\ \text{MPa}$, respectively. Such a strength was reached owing to the highest content of ZrO_2 in the tetragonal modification and

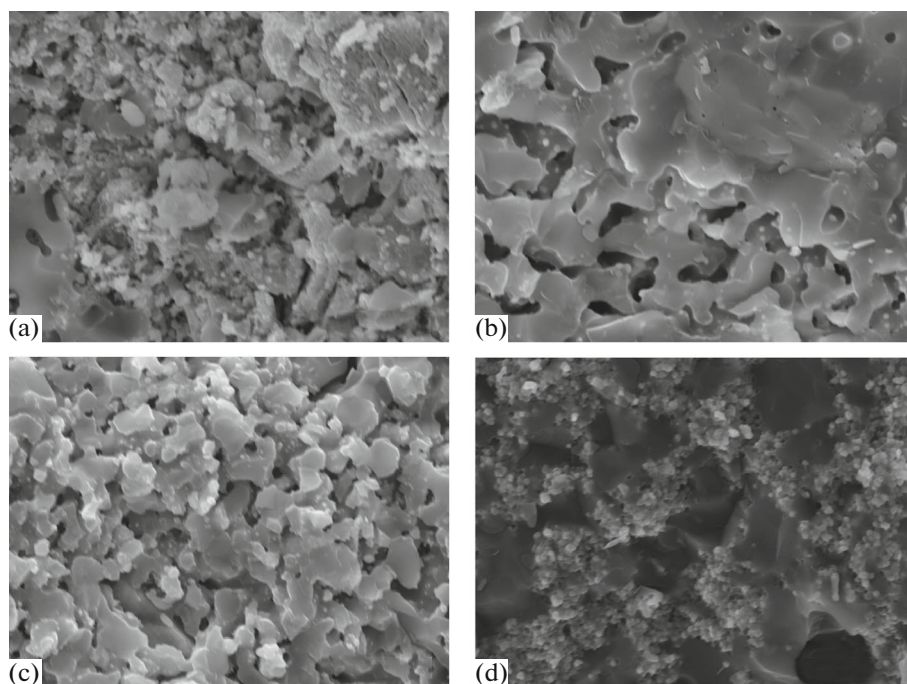


Fig. 3. Micrographs of the (a, b) 80 wt % TCP–20 wt % ZrO₂ and (c, d) 20 wt % TCP–80 wt % ZrO₂ ceramics (a, c) without and (b, d) with a sintering additive.

also to the formation of a dense sintered microstructure.

Thus, we synthesized and studied composite materials in the ZrO₂–TCP system that contained 0 to 100% ZrO₂. Owing to using a sintering additive based on Na₂SiO₃, we obtained dense composite ceramic materials containing to 80 wt % ZrO₂ with a porosity less than 2% and a flexural strength to 260 MPa. These materials were thermally stable and retained the initial phase composition, which was due to the action of the additive favoring the reduction of the sintering temperature. The materials had a uniform poreless microstructure with ZrO₂ and TCP grain sizes to 0.5 and to 5 μm, respectively. The materials we developed can be used in medicine for producing bone implants capable of withstanding high mechanical loads.

ACKNOWLEDGMENTS

This work was supported by the Council for Grants of the President of the Russian Federation for State Support of Young Russian Scientists and State Support of Leading Scientific Schools of the Russian Federation (grant no. MK–5661.2018.8, fellowship no. SP–3724.2018.4).

REFERENCES

1. Manicone, P.F., Iommetti, P.R., and Raffaelli, L., *J. Dent.*, 2007, vol. 35, no. 11, pp. 819–8262.
2. Afzal, A., *Mater. Expr.*, 2014, vol. 4, no. 1, pp. 1–12.
3. Kong, Y.M., Bae, C.J., Lee, S.H., Kim, H.W., and Kim, H.E., *Biomaterials*, 2005, vol. 26, no. 5, pp. 509–517.
4. Yu, W., Wang, X., Zhao, J., Tang, Q., Wang, M., and Ning, X., *Ceram. Int.*, 2015, vol. 41, no. 9, pp. 10600–10606.
5. Evis, Z., *Ceram. Int.*, 2007, vol. 33, no. 6, pp. 987–991.
6. Leong, C.H., Lim, K.F., Muchtar, A., and Yahaya, N., *Adv. Mater. Res.*, 2013, vol. 750, pp. 1664–1668.
7. Goldberg, M.A., Smirnov, V.V., Protsenko, P.V., Antonova, O.S., Smirnov, S.V., Fomina, A.A., Kononov, A.A., Leonov, A.V., Ashmarin, A.A., and Barinov, S.M., *Ceram. Int.*, 2017 vol. 43, no. 16, pp. 13881–13884.
8. McHale, A.E. and Roth, R.S., *Phase Equilibrium Diagrams*, Westerville (OH): Am. Ceram. Soc., 1996, vol. XII, diagrams 9898 and 9899.

Translated by V. Glyanchenko